N-Sm*A*-Sm*C* phase transitions probed by a pair of elastically bound colloids

Muhammed Rasi M,[1] K. P. Zuhail,[1] Arun Roy,[2] and Surajit Dhara[1,*]
[1]*School of Physics, University of Hyderabad, Hyderabad 500046, India*
[2]*Soft Matter Group, Raman Research Institute, Bangalore 500080, India*

(Received 2 January 2018; published 13 March 2018)

The competing effect of surface anchoring of dispersed microparticles and elasticity of nematic and cholesteric liquid crystals has been shown to stabilize a variety of topological defects. Here we study a pair of colloidal microparticles with homeotropic and planar surface anchoring across *N*-Sm*A*-Sm*C* phase transitions. We show that below the Sm*A*-Sm*C* phase transition the temperature dependence of interparticle separation (D) of colloids with homeotropic anchoring shows a power-law behavior; $D \sim (1 - T/T_{AC})^{\alpha}$, with an exponent $\alpha \approx 0.5$. For colloids with planar surface anchoring the angle between the joining line of the centers of the two colloids and the far field director shows characteristic variation elucidating the phase transitions.

DOI: 10.1103/PhysRevE.97.032702

I. INTRODUCTION

When foreign particles are dispersed in an uniformly aligned nematic liquid crystal the average orientation of the molecules (i.e., the director) is locally deformed around the particles due to the strong surface anchoring. Each particle stabilizes topological points or loop defects creating an elastic deformation in the surrounding medium [1–11]. The deformation increases the elastic energy of the liquid crystals. When the distortion regions of two physically separated particles tend to overlap they exhibit long-range elastic interaction [3,4,12,13]. The interaction energy is anisotropic and typically of the order of a few thousand $k_B T$, where k_B is the Boltzmann constant and T is the absolute temperature [2,14]. The system minimizes the total elastic energy by sharing the topological defects associated with the particles, and based on this principle various interesting two- and three-dimensional colloidal assemblies have been reported [8,13,15–19].

When the colloidal particles are dispersed in a Sm*A* liquid crystal, the situation is very different due to the translational order in addition to the orientational order of the molecules [20–28]. The surface anchoring of the Sm*A* layers at the colloid's surface is not well defined, and understanding of the induced defects and equilibrium separation among the particles is incomplete. Very recently we have shown that the surface anchoring and defects in the Sm*A* phase can be studied by dispersing the colloids in the nematic phase of a liquid crystal that exhibits *N*-Sm*A* phase transition [29–33]. In the nematic phase the well-defined anchoring of the molecules on the particle's surface guides the layer orientation and elastic deformation in the Sm*A* phase around the colloids when cooled across the *N*-Sm*A* phase transition. We showed that the point defects such as hyperbolic hedgehog and boojum defects are transformed to focal conic line defects, and the elasticity of the respective media controls the equilibrium separation between the particles.

In the Sm*C* phase the molecules are titled with respect to the layer normal, and consequently it becomes weakly biaxial due to the anisotropic fluctuations of the orientation of the long axes. There are some theoretical and experimental studies of the spherical inclusions in the Sm*C*/Sm*C** liquid crystals but mostly in free-standing films [28,34–38]. In this paper we report experimental studies on a pair of colloids with planar and homeotropic surface anchoring across the *N*-Sm*A*-Sm*C* phase transitions. Our study shows that the temperature dependence of the equilibrium separation and the angle of the colloid pair with respect to the far field director depend on the type of surface anchoring and are highly sensitive to the elasticity and Sm*C* order parameter.

II. EXPERIMENTAL

Silica microspheres of diameter 5.2 μm obtained from Bangs Chemicals (USA) were coated with octadecyldimethyl-3-trimethoxysilylpropyl-ammonium chloride (DMOAP), which provides homeotropic surface anchoring of liquid crystal molecules. The coated particles were dispersed in a liquid crystal that exhibits the following phase transitions: Cr 33.2 °C, Sm*C* 57.7 °C, Sm*A* 65.5 °C, N 68 °C I. The microspheres were coated with N-methyl-3 aminopropyl trimethoxy-silane (MAP) to induce planar anchoring of the molecules. Liquid crystal cells were made of two parallel glass plates coated with polyimide AL-1254 and rubbed in the antiparallel way for getting planar alignment of the director. Colloidal mixture was introduced into the cell of thickness in the range 11–14 μm by capillary action. A laser tweezer was built around an inverted optical polarizing microscope (Nikon Eclipse Ti-U) using a cw solid-state laser operating at 1064 nm (Aresis, Tweez 250Si). An acousto-optic deflector interfaced with a computer was used to control the trap movement. The positions of the colloids were tracked by using the video-microscopy technique with a resolution of ±10 nm [39,40].

The temperature of the sample was controlled by a proportional-integral-derivative controller (Instec Inc.) with

*sdsp@uohyd.ernet.in

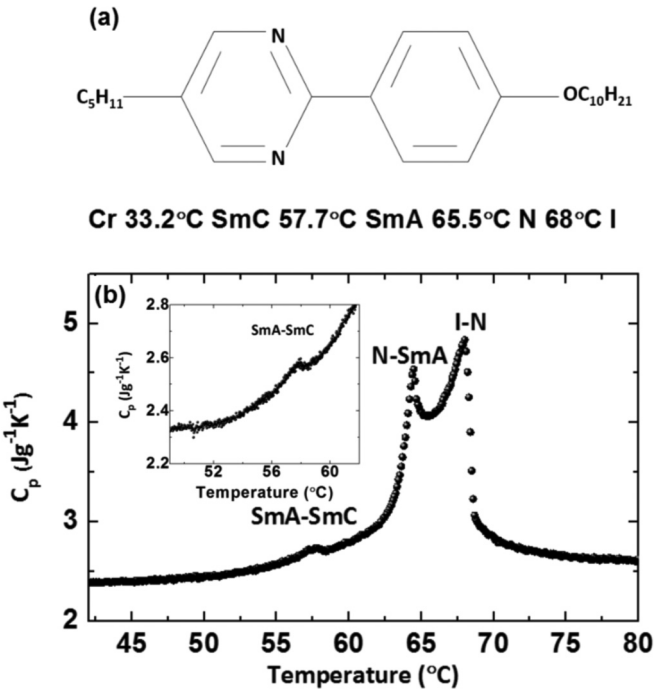

FIG. 1. (a) Molecular structure and phase transition temperatures of the compound. (b) Temperature profile of the heat capacity (C_p) on fast cooling (0.7 K/h). (Inset) Slow cooling (0.12 K/h) across the SmA-SmC phase transition.

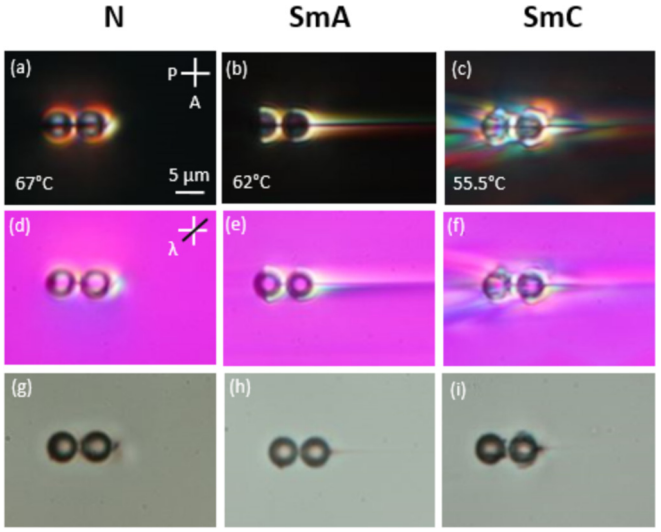

FIG. 2. Optical photomicrographs of a pair of collinear colloids with homeotropic anchoring at different temperatures in a planar cell. Images are taken (a–c) with crossed polarizers, (d–f) with crossed polarizers and a λ-plate, and (g–i) without polarizers and the λ-plate. Cell thickness and diameters of the colloids are 5.2 μm and 14 μm, respectively.

an accuracy of ±0.1 °C. The trajectories of the particles as a function of temperature were video recorded with a CCD camera at 25 frames per second while the sample was cooled at the rate of 0.2 °C/min. The x-ray diffraction studies were carried out on unoriented samples by using Cu-K_α radiation from a PANalytical instrument (DY 1042-Empyrean) and a linear detector (PIXcel 3D). The sample temperature was controlled with a precision of 0.1 °C using a Linkam heater and a temperature controller. The molecular tilt angle (θ) was calculated from the temperature-dependent layer spacing across the SmA-SmC phase transition. The chemical structure of the compound used in the experiment is shown in Fig. 1(a). The sample was obtained from Prof. R. Dabrowski, Institute of Chemistry, Military University of Technology, Warsaw, Poland. The heat capacity (C_p) measurements were made by a fully automated adiabatic scanning calorimeter. To achieve maximum insulation from the environment the air between them was removed by a vacuum pump [41]. The almost real thermal equilibrium state of the sample was achieved due to the high-temperature stability (50 mK) and the slow scanning rates. The heat capacity of the empty cell was measured in a separate experiment and subtracted from the measured data to get actual C_p of the sample.

III. RESULTS AND DISCUSSION

The variation of specific heat (C_p) across the phase transitions obtained from high-resolution ac calorimetry is shown in Fig. 1(b). It shows a first order N-SmA and second order SmA-SmC phase transitions. First we looked at the DMOAP-coated colloids in the nematic phase. It was observed that the colloids induce a Saturn ring defect (i.e., quadrupolar defect structure) irrespective of cell thickness. This is in contrast with the observation in conventional liquid crystals such as 5CB or 8CB [2,4,8,9]. Using optical tweezer we converted a few colloids from quadrupolar to dipolar structure and formed a collinear pair of elastic dipoles. The dipoles are bound by elastic forces of the liquid crystal medium with a equilibrium separation due to the elasticity of the medium and the hyperbolic hedgehog defects. An isolated dipolar pair was studied across the N-SmA-SmC phase transitions while cooling at the rate of 0.2 °C/min. Figure 2 shows some representative images of a pair of dipoles in different phases. When the temperature is decreased from the nematic to SmA phase the hyperbolic hedgehogs defects are transformed into smectic focal line defects. We reported similar results in 8CB liquid crystal in our previous study [30]. It was shown that the transformation took place through the formation of a splay soliton at the expense of energy cost associated with elastic bend deformation. The length of the defect line is extended up to to the several times the diameter of the colloid [Fig. 2(b)]. The homeotropic surface anchoring of the molecules in the SmA phase is retained only on the left-half part of the left colloid, and it is broken in the remaining part creating a strong layer distortion around the colloids. The λ-plate (530 nm) images at the corresponding temperatures are shown in Figs. 2(d)–2(f). The bluish and yellowish colors in narrow regions on the upper and lower sides of the line defect indicate that the molecules in the layers are tilted in the opposite direction creating an angle discontinuity across the defect line.

In the SmC phase the layer distortion becomes nonuniform surrounding the colloidal pair [Fig. 2(f)]. This could arise due to the random variation of tilting direction of the molecules and the weak biaxiality of SmC phase [42]. The length of the defect line in the SmC phase has decreased compared to

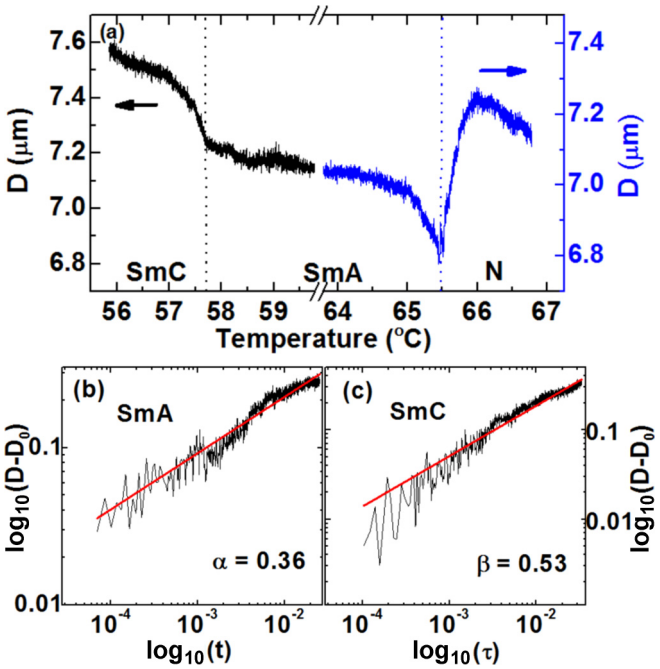

FIG. 3. (a) Temperature dependence of center-to-center separation (D) of a pair of dipolar colloids across the N-SmA-SmC phase transitions in a planar cell. Temperature variation of D below (b) the N-SmA and (c) the SmA-SmC phase transition in logarithmic scale. The red lines are the best fits to the power laws: $(D - D_0) \sim t^{\alpha}$, with an exponent $\alpha = 0.36$, where $t = (1 - T/T_{NA})$ and $(D - D_0) \sim \tau^{\beta}$, with an exponent $\beta = 0.53$, where $\tau = (1 - T/T_{AC})$. Cell thickness and the diameter of the colloids are 14 μm and 5.2 μm, respectively. The sample was cooled at a rate of 0.2 °C/min.

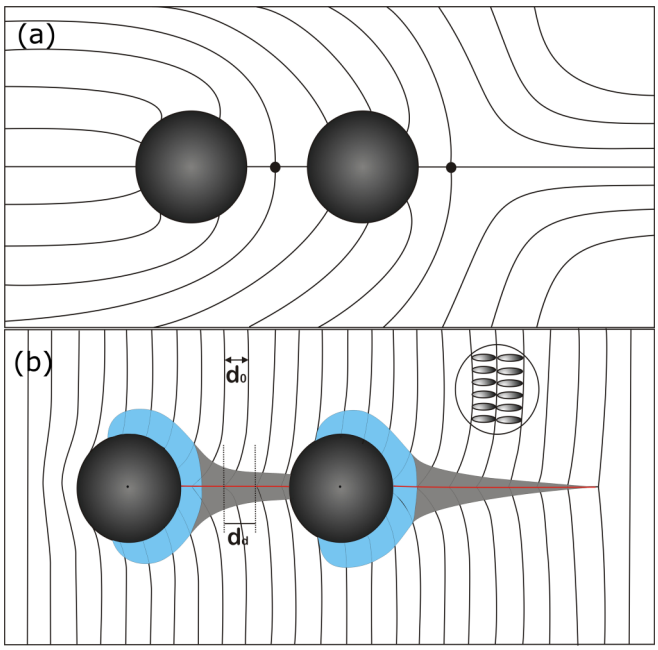

FIG. 4. (a) Schematic diagrams of two collinear colloids in the nematic phase with homeotropic surface anchoring. The continuous lines represent the director field. (b) Schematic diagram showing the layer distortion and focal conic line around the colloid pair in the SmA phase. The continuous lines represent SmA layers. Orientation of a few molecules within the layers is shown inside the circle in the upper right-hand corner. The blue regions indicate the breaking of homeotropic anchoring. The red line represents the focal conic line. The gray regions represent the deviation (or distortion) of the layers from the uniform orientation. d_d and d_0 are the thickness of the dilated and undilated layers, respectively.

that of the SmA, and the center-to-center separation is not the same in all the phases [Figs. 2(h)–2(i)]. Here we define an extrapolation length $l = W/B$, where W and B are the surface anchoring energy and elastic layer compressional modulus of the smectics, respectively. In the SmA phase [43,44], $W \sim 10^{-2}$–10^{-3} J/m^3 and $B \sim 10^5$–10^6 J/m^3 and estimated $l \sim 0.1$ μm, which is much smaller than the size of the colloids. Thus strong surface anchoring guides the transformation of the defect across the phase transition.

We measured the interparticle separation (D) across the N-SmA-SmC phase transitions as a function of temperature while cooling the sample at the rate of 0.2 °C/min as shown in Fig. 3(a). In the nematic phase D increases linearly followed by almost a discontinuous change at the N-SmA phase transition. We recently explained the pretransitional behavior of D based on the increase in the ratio of the bend to splay elastic constant (i.e., K_{33}/K_{11}) [30]. Since the equilibrium separation is governed by the elasticity of the medium, the discontinuity in D marks the discontinuity of the elastic constants of the respective phases. The distance of closest approach between the particles at the N-SmA transition (T_{NA}) is $D_0 = 6.8$ μm, and this is about 1.6 μm larger than the center-to-center distance between the two colloids (5.2 μm). This indicates that at the transition there are about 800 layers present between them assuming the length of a molecule is about 2 nm. Below the N-SmA transition D increases continuously. The temperature dependence of $D - D_0$, just below the N-SmA transition is shown in Fig. 3(b) using a logarithmic scale. It shows a power-law behavior, $(D - D_0) \sim t^{\alpha}$, with an exponent $\alpha = 0.36$, where $t = (1 - T/T_{NA})$. A similar exponent was also obtained in the case of 8CB liquid crystal [30]. In the SmA phase there is an angle discontinuity across the focal line due to the opposite tilting of the molecules. A schematic representation of this is presented in Fig. 4(b). For the purpose of comparison a schematic diagram in the nematic phase is also shown in Fig. 4(a). The blue region around the colloids in Fig. 4(b) indicates the region where the homeotropic anchoring of the director is broken to reconcile with the far field director. The angle discontinuity causes a layer dilation given by $d_d - d_0$, where d_d and d_0 are the thickness of the dilated and undilated layers respectively [21,45]. A schematic representation of such layer dilation is shown in Fig. 4(b). Consequently the elastic energy $B(1 - d_d/d_0)^2$ increases where B is the SmA elastic compression or dilation modulus. Below the N-SmA transition the elastic modulus varies as $B \sim t^{0.38}$ [43]. If the discontinuity angle exceeds a critical value, it may further create edge dislocations in the confined region [46]. In the present system the length of the defect line increases and the colloidal particles are pushed apart, thereby increasing the center-to-center separation.

As the temperature is decreased in the SmA phase D increases very slowly till the SmA-SmC transition temperature is reached [Fig. 3(a)]. For example, a small negative slope is

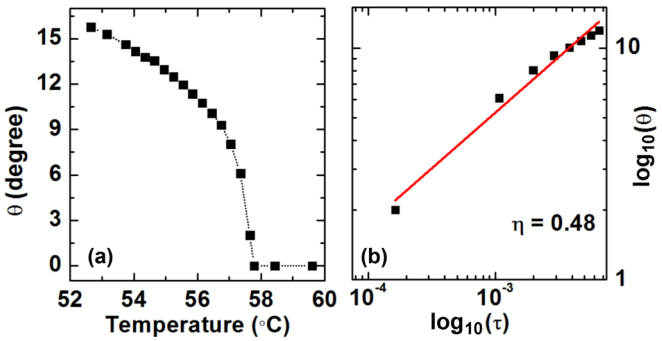

FIG. 5. (a) Temperature variation of tilt angle (θ) below the SmA-SmC phase transition. (b) Variation of θ with reduced temperature below the SmA-SmC transition (logarithmic scale) and the best fit to the equation $\theta = \theta_0 \tau^{\eta}$ with an exponent $\eta = 0.48$.

observed between 60 °C and 57.7 °C. At the transition point ($T_{AC} = 57.7$ °C), D changes slope and increases continuously as the temperature is decreased. For example, at the SmA-SmC transition temperature $D = 7.2\,\mu$m, and it is increased to 7.6 μm when the temperature is decreased to 56 °C. The N-SmA and SmA-SmC phase transitions in this compound are weakly first order and second order, respectively. It appears that the temperature dependence of D is a pointer to the discontinuous and continuous phase transitions at the respective temperatures. In Fig. 3(c) we show the temperature variation of $D - D_0$ in the SmC phase using a logarithmic scale. It can also be fitted to a power law, $(D - D_0) \sim \tau^{\beta}$, with $\beta = 0.53$, where $\tau = (1 - T/T_{AC})$. The model based on the de Gennes theory suggests that the SmA-SmC phase transition belong to the 3D XY universality class, whereas many experiments showed a classic mean-field behavior with the tilt angle θ is an order parameter which is given by $\theta = \theta_0 |\tau|^{\eta}$, where $\eta = 0.5$. To verify it we measured the temperature dependence of θ from x-ray diffraction studies, presented in Fig. 5(a). The exponent of the order parameter obtained from the fitting [Fig. 5(b)] is $\eta = 0.48$, and it is very close to the exponent $\beta = 0.53$ of the temperature dependence of D [see Fig. 3(c)]. Thus we conjecture that the interparticle separation D is coupled to the order parameter (θ) of the SmA-SmC phase transition. It may be mentioned that several physical properties such as birefringence and elastic modulus of the SmA phase shows the effect of strong pretransitional fluctuations across SmA to the tilted phase (SmC or SmC*) transition [47–50]. In the present system we do not observe any significant pretransitional effect except a small and linear variation of D just above the SmC to SmA phase transition.

When colloidal particles with planar anchoring (coated with MAP) are introduced in a planar cell, each particle creates a pair of antipodal surface defects known as boojums. Figure 6 shows some representative optical images of a pair of colloids with boojums and the transformation of the boojums across the N-SmA-SmC phase transitions. The transformation of boojums across the N-SmA phase has been studied by us recently [29]. In the SmA phase the boojums are transformed into two line defects which are extended on the opposite sides of the pair along the rubbing direction up to several micrometers. Subsequent λ-plate images [Figs. 6(d)–6(f)] clearly indicate that the SmA layers are tilted in the opposite direction of the

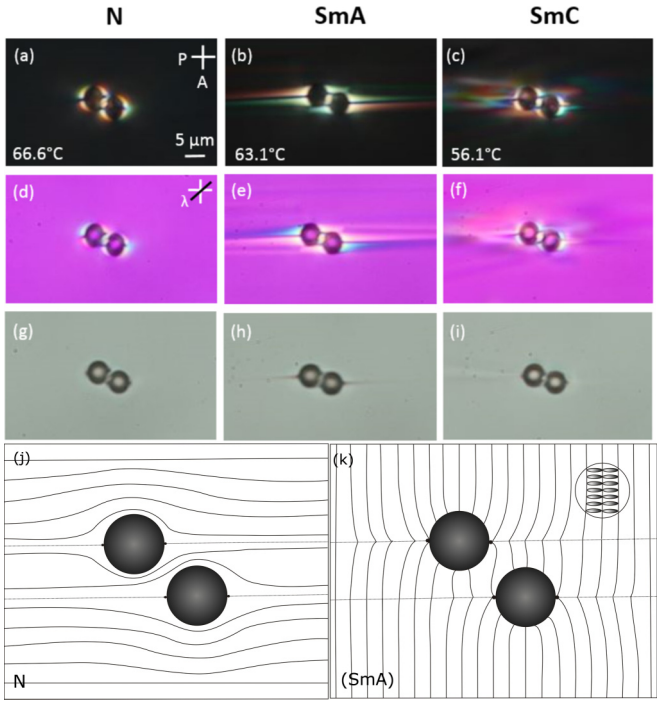

FIG. 6. Optical photomicrographs of a pair of colloids with boojums defects in a planar cell at different temperatures in the N, SmA, and SmC phases in a planar cell. Images are taken (a–c) with crossed polarizers, (d–f) with crossed polarizers and a λ-plate, and (g–i) without polarizers and the λ-plate. The diameters of the colloids and the cell thickness are 5.2 μm and 11.5 μm respectively. (j) Schematic diagram showing the director field around two colloids with planar anchoring in the nematic phase. (k) Schematic diagram showing subsequent layer orientation in the SmA phase.

defect lines. Schematic diagrams showing the director field and SmA layer orientation are shown in Figs. 6(j) and 6(k). It may be noted that in the case of homeotropic surface anchoring, in both SmA and SmC phases, the focal lines are collinear, whereas in the case of planar anchoring they are parallel to each other and are separated by a distance nearly equal to the radius of the colloidal particle. In the SmC phase, the nonuniformly colored regions around the colloids indicate that the layers are distorted randomly [Fig. 6(c)]. This could again be due to the weak biaxiality of the SmC phase as we discussed in the case of homeotropic anchoring previously [Fig. 2(c)]. In addition to this the defect lines have become shorter and less distinct than the SmA phase [Fig. 6(i)]. It suggests that the angle discontinuity in the SmC phase has decreased with respect to the SmA phase.

To see the effect of phase transitions on the interparticle separation we measured D across the N-SmA-SmC phase transition as a function of temperature, presented in Fig. 7(a). The interparticle separation D decreases very sharply followed by a slope change at the N-SmA phase transition ($T_{NA} =$ 65.5 °C) and becomes independent of temperature in the SmA phase and across the SmA-SmC transition. Hence there is no noticeable change of D across the SmA-SmC phase transition, and this is in contrast to the homeotropic colloids discussed in the previous section. In the case of planar anchoring since the line defects in the SmA and SmC phases are parallel to

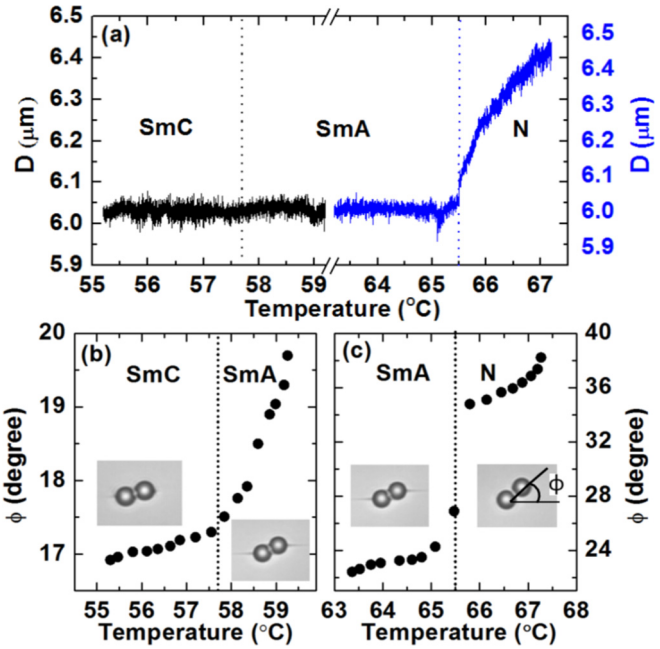

FIG. 7. (a) Temperature dependence of center-to-center separation (D) of a pair of colloids with planar anchoring in a planar cell. Temperature variation of ϕ across the (b) SmA-SmC and (c) N-SmA phase transitions. ϕ is the angle between the joining the far field director and the joining line between the two centers of the colloids (shown in inset). The sample was cooled at a rate of 0.2 °C/min. The diameters of the colloids and the cell thickness are 5.2 μm and 11.5 μm, respectively.

each other the colloids are not pushed apart unlike in the previous case [see Figs. 2(b) and 2(c)], hence D remains unchanged. This suggests that the temperature dependence of D depends on how the two colloids are bound by defects. The line joining the center-to-center of the colloids makes an angle ϕ with respect to the far field director. To see the effect of phase transitions on ϕ, we measured it as a function of temperature, presented in Figs. 7(b) and 7(c). The angle (ϕ) decreases discontinuously and continuously across the N-SmA and SmA-SmC phase transitions, respectively. For example, at the N-SmA transition [Fig. 7(c)], ϕ discontinuously decreases from 19° to 17.5°. Across the SmA-SmC transition [Fig. 7(b)] ϕ decreases continuously with a change of slope at the phase transition temperature (57.7 °C). Hence in the case of homeotropic surface anchoring D is sensitive to both the N-SmA and SmA-SmC phase transitions. In the case of planar surface anchoring D is sensitive only to N-SmA transition, whereas ϕ is sensitive to both the N-SmA and SmA-SmC phase transitions. The structural change that directly affects the colloid pair across the SmA-SmC transition is the molecular tilt angle (θ), which is the order parameter of the SmA-SmC phase transition. Therefore, it is expected that the relative variation of D and ϕ across the phase transitions is connected to the order parameters of the respective phase transitions. Theoretical and computer simulation studies could be useful for understanding the direct linking of these physical quantities.

IV. CONCLUSION

We have studied a pair of spherical colloids with homeotropic and planar surface anchoring across N-SmA-SmC phase transitions. The hyperbolic point defect is transformed to a smectic focal line below the N-SmA transition. The line defect is slightly shortened without any significant change in the structure below the SmA-SmC transition. The temperature dependence of the interparticle separation of a collinear colloids shows a similar power-law as that of SmA-SmC order parameter. For colloids with planar surface anchoring there is no observable change in the interparticle separation across the SmA-SmC transition, although the angle made by the joining line with respect to the far field director decreases continuously with a characteristic slope change. This suggests that the interparticle separation of a pair of colloids and their orientation angle are coupled to the order parameters of the phase transitions.

ACKNOWLEDGMENTS

We gratefully acknowledge support from the Department of Science and Technology, Govt. of India (DST/SJF/PSA-02/2014-2015), and DST-PURSE. M.R.M acknowledges DST for support through a fellowship grant. We thank Prof. Dabrowaski for providing the sample. We also thank George Cordoyiannis for helping us by doing the *ac* calorimetry measurements.

[1] P. Poulin, H. Stark, T. C. Lubensky, and D. A. Weitz, Science **275**, 1770 (1997).
[2] I. Muševič, M. Škarabot, U. Tkalec, M. Ravnik, and S. Žumer, Science **313**, 954 (2006).
[3] H. Stark, Phys. Rep. **351**, 387 (2001).
[4] R. P. Trivedi, D. Engstrom, and I. I. Smalyukh, J. Opt. **13**, 044001 (2011).
[5] O. V. Kuksenok, R. W. Ruhwandl, S. V. Shiyanovskii, and E. M. Terentjev, Phys. Rev. E **54**, 5198 (1996).
[6] P. Poulin, V. Cabuil, and D. A. Weitz, Phys. Rev. Lett. **79**, 4862 (1997).
[7] T. C. Lubensky, D. Pettey, N. Currier, and H. Stark, Phys. Rev. E **57**, 610 (1998).
[8] I. Muševič, Liq. Cryst. Today **19**, 2 (2010).
[9] I. Muševič, *Liquid Crystals Colloids* (Springer International Publishing, Switzerland, 2017).
[10] U. Tkalec and I. Musevic, Soft Matter **9**, 8140 (2013).
[11] C. P. Lapointe, S. Hopkins, T. G. Mason, and I. I. Smalyukh, Phys. Rev. Lett. **105**, 178301 (2010).
[12] R. W. Ruhwandl and E. M. Terentjev, Phys. Rev. E **56**, 5561 (1997).
[13] S. Park, Q. Liu, and I. I. Smalyukh, Phys. Rev. Lett. **117**, 277801 (2016).
[14] Y. Gu and N. L. Abbott, Phys. Rev. Lett. **85**, 4719 (2000).
[15] A. Nych, U. Ognysta, M. Skarabot, M. Ravnik, S. Zumer, and I Musevic, Nat. Commun. **4**, 1489 (2013).

[16] B. Senyuk, Q. Liu, S. He, R. D. Kamien, R. B. Kusner, T. C. Lubensky, and I. I. Smalyukh, Nature (London) **493**, 200 (2013).
[17] Q. Liu, B. Senyuk, M. Tasinkevych, and I. I. Smalyukh, Proc. Natl. Acad. Sci. U. S. A. **110**, 9231 (2013).
[18] Q. Liu, P. J. Ackerman, T. C. Lubensky, and I. I. Smalyukh, Proc. Natl. Acad. Sci. U. S. A. **113**, 10479 (2016).
[19] J. Dontabhaktuni, M. Ravnik, and S. Zumer, Proc. Natl. Acad. Sci. U. S. A. **111**, 2464 (2014).
[20] S. P. Schlotthauer, V. M. Turrion, C. K. Hall, M. G. Mazza, and M. Schoen, Langmuir **33**, 2222 (2017).
[21] C. Blanc and M. Kleman, Eur. Phys. J. E **4**, 241 (2001).
[22] M. J. Gim, D. A. Beller, and D. K. Yoon, Nat. Commun. **8**, 15453 (2017).
[23] R. Pratibha, W. Park, and I. I. Smalyukh, J. Appl. Phys. **107**, 063511 (2010).
[24] N. M. Silvestre, P. Patrício, and M. M. Telo da Gama, Phys. Rev. E **74**, 021706 (2006).
[25] C. Bohleya and R. Stannarius, Eur. Phys. J. E **20**, 299 (2006).
[26] G. Liao, I. I. Smalyukh, J. R. Kelly, O. D. Lavrentovich, and A. Jakli, Phys. Rev. E **72**, 031704 (2005).
[27] M. Selmi, J. C. Loudet, P. V. Dolganov, T. Othman, and P. Cluzeau, Soft Matter **13**, 3649 (2017).
[28] C. Bohley and R. Stannarius, Soft Matter **4**, 683 (2008).
[29] K. P. Zuhail and S. Dhara, Appl. Phys. Lett. **106**, 211901 (2015).
[30] K. P. Zuhail, P. Sathyanarayana, D. Seč, S. Čopar, M. Škarabot, I. Muševič, and Surajit Dhara, Phys. Rev. E **91**, 030501(R) (2015).
[31] K.P. Zuhail, S. Čopar, I. Muševič, and S. Dhara, Phys. Rev. E **92**, 052501 (2015).
[32] K. P. Zuhail and S. Dhara, Soft Matter **12**, 6812 (2016).
[33] R. Sahoo and S. Dhara, Liq. Cryst. **44**, 1582 (2017).
[34] M. Tasinkevych and D. Andrienko, Cond. Mat. Phys. **13**, 33603 (2010).
[35] M. Tasinkevych, N. M. Silvestre, and M. M. Telo da Gama, New. J. Phys. **14**, 073030 (2012).
[36] P. Cluzeau, P. Poulin, G. Joly, and H. T. Nguyen, Phys. Rev. E **63**, 031702 (2001).
[37] P. V. Dolganov and V. K. Dolganov, Phys. Rev. E **73**, 041706 (2006).
[38] P. Cluzeau, V. Bonnand, G. Joly, V. Dolganov, and H. T. Nguyen, Eur. Phys. J. E **10**, 231 (2003).
[39] M. V. Rasna, K. P. Zuhail, U. V. Ramudu, R. Chandrasekar, and S. Dhara, Phys. Rev. E **94**, 032701 (2016).
[40] M. V. Rasna, U. V. Ramudu, R. Chandrasekar, and S. Dhara, Phys. Rev. E **95**, 012710 (2017).
[41] J. Thoen, G. Cordoyiannis, and C. Glorieux, Liq. Cryst. **36**, 669 (2009).
[42] P. G. de Gennes and J. Prost, *The Physics of Liquid Crystals* (Oxford University Press, New York, 1995).
[43] M. Benzekri, J. P. Marcerou, H. T. Nguyen, and J. C. Rouillon, Phys. Rev. B **41**, 9032 (1990).
[44] Z. Li and O. D. Lavrentovich, Phys. Rev. Lett. **73**, 280 (1994).
[45] C. Blanc and M. Kleman, Eur. Phys. J. B **10**, 53 (1999).
[46] J. Jeong and M. W. Kim, Phys. Rev. Lett. **108**, 207802 (2012).
[47] J. Fernsler, D. Wicks, D. Staines, A. Havens, and N. Paszek, Liq. Cryst. **39**, 1204 (2012).
[48] M. Škarabot, K. Kočevar, R. Blinc, G. Heppke, and I. Muševič, Phys. Rev E **59**, R1323(R) (1999).
[49] S. Shibahara, J. Yamamoto, Y. Takanishi, K. Ishikawa, and H. Takezoe, Phys. Rev E **62**, R7599(R) (2000).
[50] S. Shibahara, J. Yamamoto, Y. Takanishi, K. Ishikawa, H. Takezoe, and H. Tanaka, Phys. Rev. Lett. **85**, 1670 (2000).